

Intermolecular Dearomative [4+2] Cycloaddition of Naphthalenes via Visible-Light Energy-Transfer-Catalysis

Pramod Rai,[‡] Kakoli Maji,[‡] Sayan K. Jana,[‡] Biplab Maji*

Department of Chemical Sciences, Indian Institute of Science Education and Research Kolkata, Mohanpur 741246, India.

ABSTRACT: Dearomative cycloaddition reaction serves as a blueprint for creating three-dimensional molecular topology from flat-aromatic compounds. However, severe reactivity and selectivity issues make this process challenging. Herein, we describe visible-light energy-transfer catalysis for the intermolecular dearomative [4+2] cycloaddition reaction of feed-stock naphthalene molecules with vinyl benzenes. Tolerating a wide range of functional groups, a variety of structurally diverse 2-acyl naphthalenes and styrenes could easily be converted to a diverse range of bicyclo[2.2.2]octa-2,5-diene scaffolds in high yields and selectivities. The late-stage modification of pharmaceutical agents further demonstrated the broad potentiality of this methodology. The efficacy of the introduced methods was further highlighted by the post-synthetic diversification of the products. Furthermore, photoluminescence, electrochemical, kinetic, and control experiments support the energy transfer catalysis

Constructing three-dimensional (3D) molecular scaffolds from two-dimensional (2D) molecules is highly challenging yet significantly impacts organic synthesis and drug discovery programs.¹⁻⁴ The cycloaddition reactions that convergently and predictably join multiple molecular fragments have been recognized as a powerful tool for this purpose (Figure 1).⁵⁻⁸ Notably, in [4+2] cycloaddition reaction, two new σ -bonds, and one π -bond are formed in a 3D six-membered ring topology from two simple unsaturated reaction components, *diene*, and *dienophile* (Figure 1a).^{9,10} In fact, this thermally allowed process has been a fundamental reaction type demonstrating its molecular complexity generating power for many years.¹¹⁻¹³ In this context, polycyclic aromatic hydrocarbon such as naphthalene also contains alternating double bonds. Besides, they are abundant and inexpensive feed-stock chemicals (present at about 10% in typical coal tar).¹⁴ However, these 2D molecules displayed limited application in 3D complexity generating cycloadditions reactions due to severe challenges associated with breaking the increased stabilization conferred by aromaticity (resonance energy = 80.3 kcal mol⁻¹) and selectivity (Figure 1b,c).^{15,16} A typical thermal dearomative [4+2] cycloaddition with naphthalenes required harsh reaction conditions (high temperature up to 210 °C, pressure up to 10³ atm),¹⁷ specially designed reaction conditions,¹⁸⁻²⁰ or reactive *dienophile*^{21,22} (hereafter called *arenophile*) to overcome the high kinetic barrier (Figure 1c).^{23,22,24} However, since the free energy is often positive for such a reaction, the reverse reaction is thermodynamically preferred resulting in lower product yields (Figure 1d, blue curve).^{19,25} Photochemistry provides alternative strategies for achieving challenging and unusual chemical transformations in this context.^{23,26,27} However, since most organic molecules are incapable of absorbing visible light efficiently, direct high-energy ultraviolet (UV) light irradiation is required. Indeed, the UV-light mediated dearomative [4+2] cycloaddition with naphthalenes is known.^{28,29} However, their utility in organic synthesis is minimal due to the requirement of specific *arenophiles*, meager product yields, and unpredictable side reactions conferred by UV light (Figure 1c). Eliminating UV irradiation should ideally broaden the synthetic applicability of this process with enriched structural diversity. The recent renaissance of visible-light photocatalysis provides a new space for dearomative [4+2] cycloaddition reaction *via* sensitization induced energy transfer (EnT) catalysis^{30,31} or direct visible-light excitation of the *dienophile* in some cases.²³ Conceptually, the EnT process can selectively excite a ground state of a polycyclic hydrocarbon by using an appropriate photosensitizer to a higher triplet state (naphthalenes exhibit E_TS of 54–60 kcal mol⁻¹),³² lowering the kinetic barriers significantly compared to thermal processes (Figure 1d, black curve).³³ Furthermore, the milder reaction conditions and substantially higher E_T of the dearomatized product prevent the reverse reaction resulting in higher product yields.

Recently, Glorius and coworkers demonstrated dearomative [4+2] cycloaddition of pyridines (intramolecular)³⁰ and bicyclic azaarenes (intermolecular, Figure 1e)³³ *via* visible-light EnT catalysis. A stoichiometric Brønsted acid additive was shown to play a vital role in the latter reaction to increase the reactivity of quinolines' triplet state toward olefins.³¹ You and coworkers reported intramolecular dearomative cycloaddition of indole tethered naphthalenes (Figure 1f).³⁴ The dearomative intramolecular [2+2] cycloaddition of 1-naphthol derivatives *via* visible-light EnT catalysis was recently developed by Glorius.³⁵ The intramolecularity prepaid the entropic requirements for the last two reactions. Besides, various groups demonstrated the application of the EnT process in diverse chemical transformations.³⁶⁻⁶² However, to the best of our knowledge, intermolecular dearomative [4+2] cycloaddition reactions of naphthalenes with unactivated alkenes have not been documented yet. Herein,

we report our initial results on visible-light EnT mediated dearomative [4+2] cycloaddition of naphthalenes with styrenes to access bicyclo[2.2.2]octa-2,5-diene scaffolds (Figure 1g).

We commenced the visible-light mediated dearomative [4+2] cycloaddition reaction using 2-acetyl naphthalene **1** and 1-fluoro-4-vinyl benzene **2** as the model substrates (Table 1, Tables S1-S6). Pleasingly, the irradiation of blue light-emitting diodes ($\lambda_{\text{max}} = 427$ nm) in the presence of commercially available photosensitizer Ir[(dFCF₃ppy)₂dtbbpy]PF₆ (**PC1**, 1 mol%) in acetonitrile solution of **1** and **2** (in stoichiometric ratio) at room temperature resulted in the formation of the desired [4+2] cycloadduct **3** in 98% yield in 2:1 diastereomeric ratio, favoring *endo* (entry 1).

Notably, the regioisomeric product **4** resulting from the *syn* attack of the alkene to the 6-membered aromatic ring was not observed by ¹H nuclear magnetic resonance analysis of the crude reaction mixture. The *ortho* and *meta* cycloaddition products (Figure 1b) were also undetected in a measurable amount. We then followed the kinetics of the reaction *via* ¹H NMR spectroscopy (Figure S18). The rate of formation of **3** was found to be almost equal to the disappearance of **1** (Figure S19). This supports the direct formation of [4+2] cycloadduct **3** without the intermediacy of an [2+2] adduct as previously been observed for the intramolecular reaction.³⁴

Product **3** was computed to be thermodynamically uphill (Figure S21). However, it can be purified by flash chromatography on silica gel and was found to be stable when heated at 60 °C for 24 h. The structure of *endo*-**3** was confirmed by single-crystal X-ray crystallography.⁶³ Control experiments confirm that the light source and photosensitizer were necessary for this [4+2] cycloaddition reaction, and their absence led to no product formation (entries 2–3). As anticipated, the reaction does not provide any product formation when heated at 150 °C for 24 h (entry 4).

We then stride forward to gain more insights into the EnT mediated dearomative [4+2] cycloaddition reaction (Figure 2). The cyclic voltammetry analysis suggested that an electron transfer from the excited **PC1** ($E_{1/2}\text{Ir(III)*}/\text{Ir(IV)} = -0.89$ V *vs* SCE) to either **1** or **2** (reduction potentials $E_{1/2} = -1.81$ V and -1.42 V *vs* SCE, respectively) is not thermodynamically feasible (Figure 2a). Similarly, an oxidative quenching of the excited **PC1** ($E_{1/2}\text{Ir(III)*}/\text{Ir(II)} = 1.21$ V *vs* SCE) can also be ruled out. However, the Stern-Volmer analysis shows that 2-acetyl naphthalene **1** efficiently quenches the luminescence emission of the excited photosensitizer (Stern-Volmer quenching constant $k_q = 1.6 \times 10^4$ M⁻¹s⁻¹) (Figure 2b, c). In comparison, vinyl benzene **2** quenched the excited **PC1** at a lower rate (figure 2c). On the other hand, we have computed the S₀-T₁ gap for **1** and **2** using B3LYP/6-311+G(2d,p) level of density functional theory (Figure S20). The calculated triplet energies E_T = 55.1 kcal mol⁻¹ for **1** and 57.9 kcal mol⁻¹ for **2** are in good agreement with the previously reported values.⁵⁸ Accordingly, the triplet energy transfer from the photoexcited **PC1** (E_T = 60.1 kcal mol⁻¹)³⁹ to substrate **1** is more likely.

The reaction was also found to be amenable to some triplet-energy sensitizers, albeit at lesser efficiencies (Table 1, entries 5–9). However, a direct correlation between the E_Ts of the catalysts and product yields could not be drawn.⁴³ To gain more insight into the interaction of other photosensitizers with the substrates **1** and **2** and their efficiencies in catalyzing the EnT mediated cycloaddition reaction, we have performed the luminescence quenching experiments with Ir(ppy)₃ (**PC3**) and 4CzIPN (**PC5**). Both the catalysts give a moderate to low yield of **3**. We have found both **1** and **2** do not interact with the excited **PC3** at an appreciable rate (Figure 2d). The luminescence intensity of excited **PC5** is moderately quenched by increasing the concentration of **1** ($k_q = 0.30 \times 10^4$ M⁻¹s⁻¹) (Figure 2e). However, **2** does not communicate with the excited **PC5**. In addition, it was confirmed that an electron donor-acceptor complex between **1** and **2** does not occur, as evidenced by the lack of a change in the UV/vis spectrum (Figure 2f). The absorption spectrum of **2** possesses small residual absorption at 370 nm (molar absorptivity $\epsilon = 48.1$ M⁻¹cm⁻¹ at 370 nm). However, direct irradiation using 370 nm Kessil LEDs (emission spectral window of ~360 to ~410 nm) only gave a 35% yield of **3** (d.r. = 2:1) (Figure 2g). These results additionally suggest that the photochemical dearomative cycloaddition reaction of **1** is more efficiently triggered upon energy transfer from the excited **PC1**. Additionally, complete inhibition of the dearomative [4+2] cycloaddition reaction under oxygen (a well-known E_T quencher) further supported the triplet energy transfer process (figure 2h).

Based on the observations outlined above and the literature report, it is proposed that the photosensitizer upon visible-light excitation produces its long-lived triplet excited state. The naphthalene **1** is then activated via EnT to afford triplet intermediate **1** (T₁). The latter is then engaged in [4+2] cycloaddition with styrene **2** to yield the cycloadduct **3** *via* radical capture, intersystem crossing (ISC), and bond formation (Figure 2i).

The orbital coefficients of the relevant frontier molecular orbitals were examined to understand the origin of regioselectivity (see page S67-S68). The preferential formation of **3** can approximately be conceptualized considering the maximum interaction between the largest orbital components in the triplet intermediate **1** (T₁) and the lowest unoccupied molecular orbital of **2**. However, a detailed computational elaboration is necessary.

Finally, we explored the generality, and synthetic utility of the EnT mediated dearomative [4+2] cycloaddition reaction (Figure 3). First, the scalability of our protocol was tested for a 1.0 mmol scale reaction between **1** and **2** that provided 0.25 g

(84% yield) of **3** with the same diastereoselectivity. Then, the scope of the *arenophile* was investigated. Halogenated (F, Cl, Br) styrenes were noticed to be excellent coupling partners, yielding bicyclo[2.2.2]octa-2,5-diene scaffolds **3-8** in high yields and selectivities. The electronic nature of the substituents does not perturb the reaction. Vinyl benzenes with both electron-withdrawing (CF₃) and electron-donating substituents (OMe, OAc, Me, SMe) at different positions of the aryl ring participated in this reaction in equal efficiencies. The adducts **9-16** were obtained in 25-80% yields with a similar diastereomeric ratio. Interestingly, vinyl naphthalene could also be utilized as an *arenophile*, and the adduct **17** was isolated in 39% yield. It indicated selective energy transfer to **1**. Notably, vinyl biphenyls containing diverse electronic substituents, heteroarenes, and 4-vinyl pyridines were compatible with this reaction, and the dearomative [4+2] cycloadducts **18-20** were obtained in moderate to good yields. However, α - and β -methyl styrene fails to deliver the product in synthetically useful yields under these conditions. Pleasingly, the reaction was compatible with styrene derivatives of drug molecules, including gemfibrozil, clofibrilic acid, fenbufen, ketoprofen, and oleic acid. The adducts **21-25** were isolated in 64-80% yields and moderate diastereoselectivities. It highlighted the functional group compatibility and synthetic utility of the process for late-stage diversification of these molecules.

The scope of naphthalene derivatives was then tested. Acyl naphthalenes with diverse alkyl chains participate in this EnT mediated [4+2] cycloaddition reaction, delivering the adducts **26-28** in high yields and selectivities. Naphthalenes containing cyclic alkyl groups, including cyclobutene **29** and cyclopropane **30**, were also viable reaction partners. A CC-bond cleavage in strained cyclopropane rings was not observed. In comparison, Brown recently discovered EnT mediated CC-bond cleavage in bicyclo[1.1.0]butyl naphthyl ketone for $[2\pi + 2\sigma]$ cycloaddition reactions with styrenes.⁶⁴ Severe ring strain in the caged molecule can be reasoned responsible. *N*-Methyl imidazole bearing keto naphthalene performed well in this reaction **31**. The structures of both the *endo*- and *exo*-diastereomers were assigned by single-crystal X-ray crystallography.⁶³ Interestingly, 2-carboxyalkyl naphthalenes also smoothly undergo visible-light mediated dearomative cycloaddition reaction providing high 80-85% yields of the cycloadducts **32-34**, albeit in a moderate diastereomeric ratio. The reaction was also compatible with the naphthalene derivatives of (-)-menthol **35**, (-)-borneol **36**, and cholesterol **37**. It again highlights the utility of the visible-light-driven dearomatization reaction.

To further demonstrate the synthetic application of the [4+2] dearomative cycloaddition reaction, we have performed the derivatization of the cycloadduct *endo*-**3** to obtain complex 3D molecular architecture. The palladium-catalyzed reduction of the α,β -unsaturated double bond of *endo*-**3** in the presence of diphenyl silane gave the saturated product **38** in 52% yield in >20:1 d.r. NOE spectroscopy confirmed the stereochemical assignment. Furthermore, a Michael addition of *N*-Boc-L-cysteine methyl ester delivered the adduct **39** in 56% yield and 2:1 d.r. Notably, the Corey-Chaykovsky cyclopropanation of *endo*-**3** exclusively offered the cyclopropane **40** in 63% yield, >99:1 d.r. Similarly, the epoxidation of *endo*-**3** in the presence of H₂O₂/NaOH delivered the epoxide **41** in 70% isolated yield as a single diastereomer.

In conclusion, a new strategy for intermolecular dearomative [4+2] cycloaddition reaction of abundant aromatic compound naphthalene was developed. The reaction operates via visible-light energy transfer utilizing a commercially available sensitizer. Diverse bicyclo[2.2.2]octa-2,5-diene scaffolds were synthesized in high yields. The reaction can be scaled-up and is amicable for late-stage modification of various bioactive molecules. The ease of post-synthetic diversifications adds to the utility of the introduced method. Photoluminescence, electrochemical, kinetic, and control experiments helped understand the features of this visible-energy transfer catalysis. We anticipate that the protocol will further illuminate the EnT catalysis for designing complex molecular scaffolds. Further research exploring the reaction scope and mechanisms is currently underway in this laboratory.

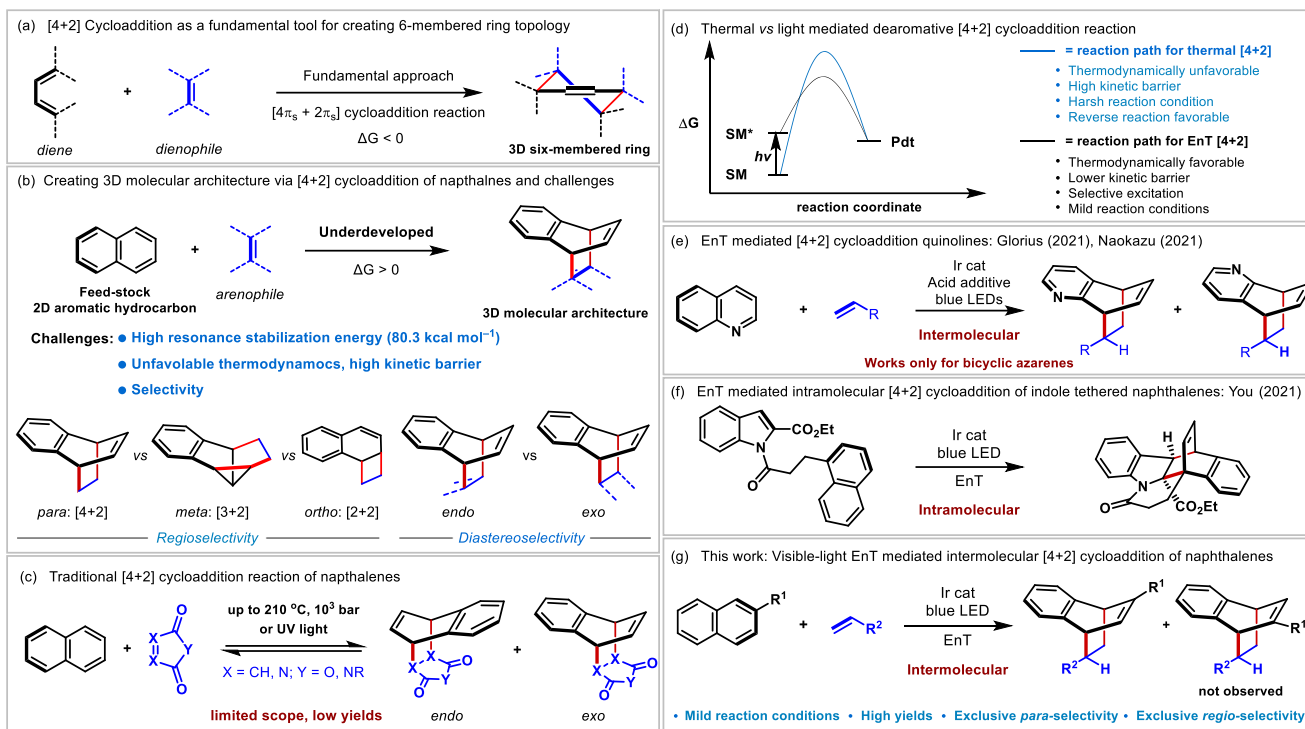
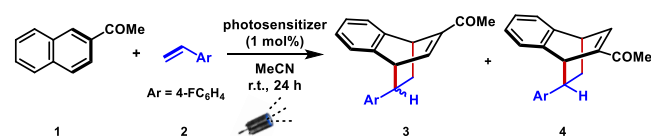


Figure 1. (a-b) Creating molecular complexity via [4+2] cycloaddition reaction and their challenges. (c) Traditional [4+2] cycloaddition reaction with naphthalenes. (d) Thermal vs light-mediated cycloaddition reaction. (e-f) EnT mediated [4+2] cycloaddition reaction of bicyclic azarenes and indole tethered naphthalenes. (g) This work: Visible-light EnT mediated intermolecular [4+2] cycloaddition reaction of naphthalenes. SM = Starting material. Pdt = Product.

Table 1. Key Reaction Optimization.^a



entry	photosensitizer (PC)	E _T (kcal/mol), hν _{max} (LED)	yield of 3 % ^b	d.r. ^b
1	Ir[(dFCF ₃ ppy) ₂ dtbbpy] PF ₆ (PC1)	60.1, 427	98 (90)	2:1
2	-	-	<5	-
3 ^c	PC1	60.1, 427	<5	-
4 ^d	PC1	60.1, 427	<5	-
5 ^e	Xanthone (PC2)	74, 370	51	1.3:1
6	Ir(ppy) ₃ (PC3)	58.1, 427	25	2:1
7	Ir[(ppy) ₂ bpy]PF ₆ (PC4)	53.1, 427	30	2:1
8 ^e	4CzIPN (PC5)	53, 427	50	1.5:1
9	Ir[(ppy) ₂ dtbbpy]PF ₆ (PC6)	49.2, 427	45	2:1

^aReaction conditions: **1** (0.1 mmol), **2** (0.12 mmol), sensitizer (1 mol%), CH₃CN (1 mL), blue LED irradiation under N₂ at r.t., 24 h. ^bYield and d.r. of **3** were determined by ¹H NMR analysis by using trimethoxy benzene as an internal standard. Isolated yield in the parenthesis. ^cAt dark. ^dAt dark at 150 °C. ^e5 mol% sensitizer is used.

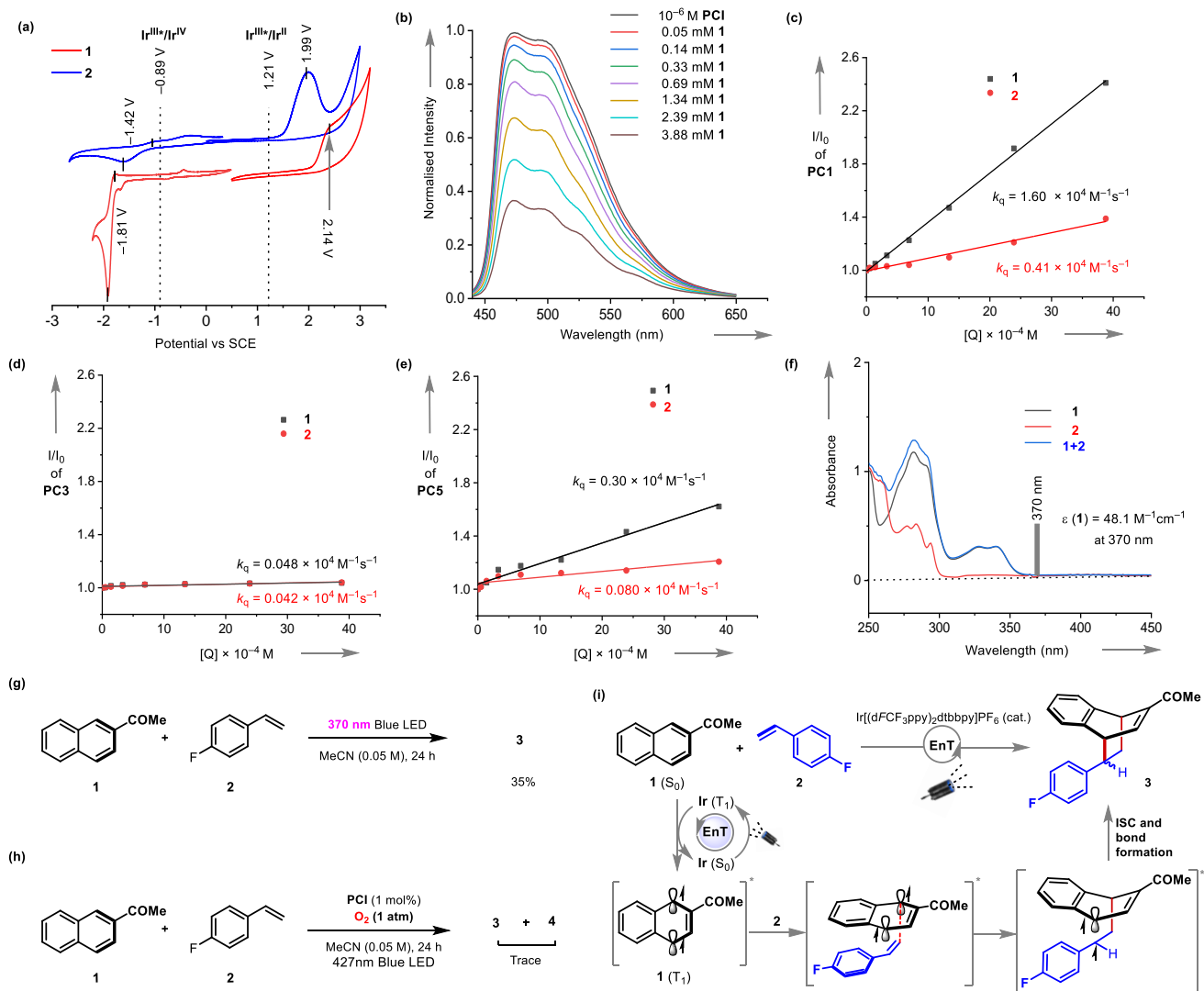


Figure 2. Mechanistic Studies and proposed mechanism. (a) Cyclic voltammety studies. (b) Decrease in luminescence intensity of **PC1** upon addition of **1**. The Stern-Volmer plot of the luminescence quenching for (c) **PC1**, (d) **PC3**, (e) **PC5**. (f) UV-Vis studies. (g) Direct excitation of **1** in the absence of photosensitizer. (h) Oxygen quenching experiments (i) Proposed mechanism.

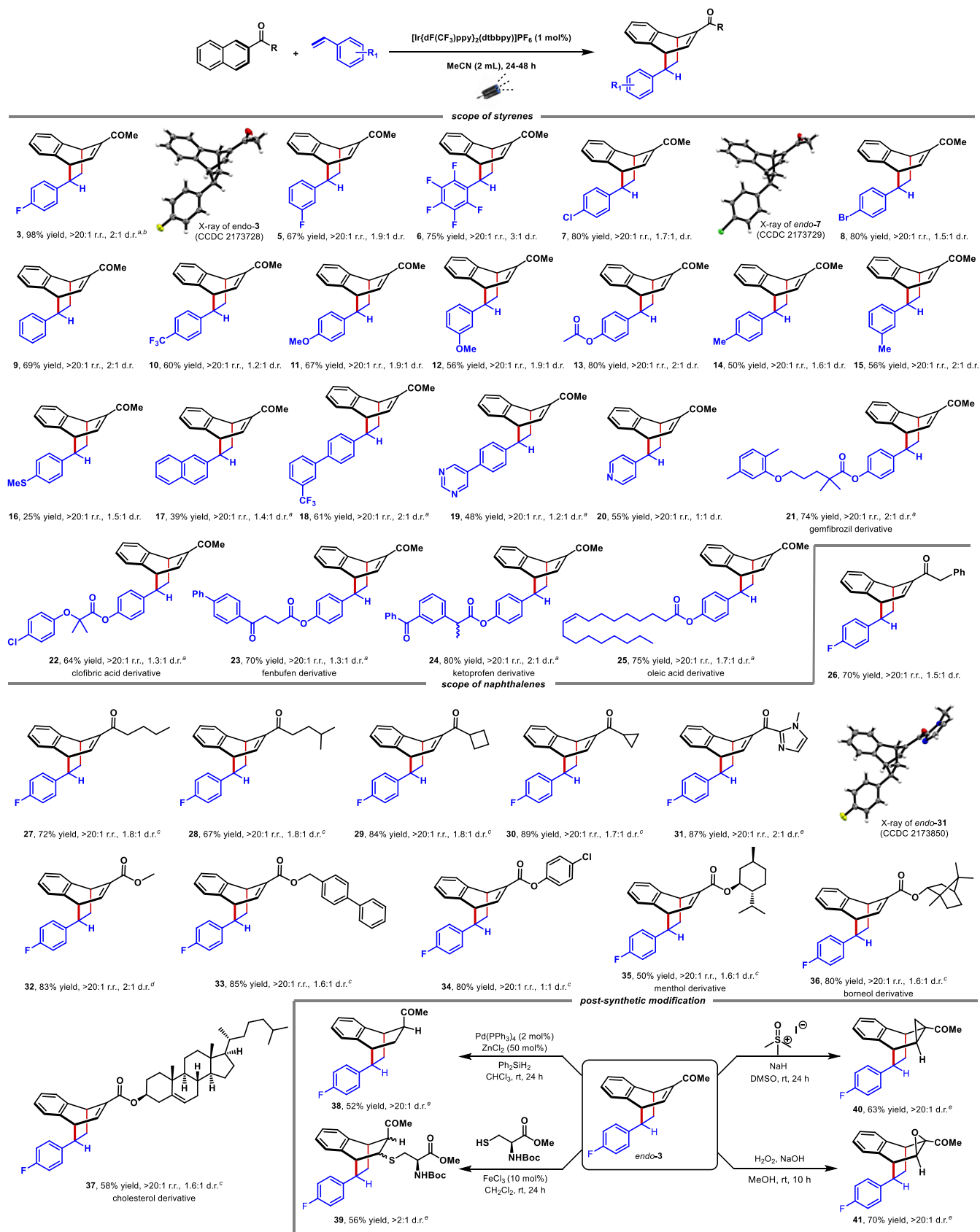


Figure 3. Synthetic utility of EnT mediated [4+2] cycloaddition reaction. Reaction conditions: Table 1, entry 1. Reaction performed in 2 mL MeCN. d.r. of products were determined by ¹H NMR analysis using 1,3,5-trimethoxy benzene as internal standard. Combined yields are given. Isolated yields of each diastereomer are provided in the SI. CCDC information ref.⁶³ ^aReaction performed in 1 mL MeCN. ^b0.246 g, 84% yield, >20:1 r.r., 1.6:1 d.r. when performed in 1 mmol scale. ^cReaction carried out for 48 h. ^dReaction carried out in MeOH solvent. ^ed.r. from the isolated product. r.r. = regioisomeric ratio. d.r. = diastereomeric ratio.

Supporting Information

The Supporting Information is available. Synthesis, crystallography, computation and characterization details (PDF)

Author information

Pramod Rai – Department of Chemical Sciences, Indian Institute of Science Education and Research Kolkata, Mohanpur 741246, India; orcid.org/0000-0002-3334-1536

Kakoli Maji – Department of Chemical Sciences, Indian Institute of Science Education and Research Kolkata, Mohanpur 741246, India; orcid.org/0000-0002-1090-536X

Sayan K. Jana – Department of Chemical Sciences, Indian Institute of Science Education and Research Kolkata, Mohanpur 741246, India; orcid.org/0000-0002-3926-6709

Biplab Maji – Department of Chemical Sciences, Indian Institute of Science Education and Research Kolkata, Mohanpur 741246, India; orcid.org/0000-0001-5034-423X; Email: bm@iiserkol.ac.in

Author Contributions

‡These authors contributed equally.

Acknowledgment

PR, KM, and SKJ acknowledge DST-INSPIRE, IISER Kolkata, and PMRF for Ph.D. fellowship, respectively. BM thanks SERB (Grant No. CRG/2019/001232) and IISER K for financial support. The authors thank Prof. A. K. Roy (IISER K) for helpful discussions.

References

1. Vardanyan, R. S.; Hruby, V. J., 10 - Antiparkinsonian Drugs. In *Synthesis of Essential Drugs*, Elsevier: 2006.
2. Raveglia, L. F.; Giardina, G. A., Accelerating the drug-discovery process: new tools and technologies available to medicinal chemists. *Future Med. Chem.* **2009**, *1*, 1019-1023.
3. Nicolaou, K. C.; Edmonds, D. J.; Li, A.; Tria, G. S., Asymmetric Total Syntheses of Platensimycin. *Angew. Chem. Int. Ed.* **2007**, *46*, 3942-3945.
4. Roche, S. P.; Porco Jr., J. A., Dearomatization Strategies in the Synthesis of Complex Natural Products. *Angew. Chem. Int. Ed.* **2011**, *50*, 4068-4093.
5. Carruthers, W., *Cycloaddition Reactions in Organic Synthesis*. Elsevier Science: 2013.
6. Kobayashi, S.; Jørgensen, K. A., Cycloaddition Reactions in Organic Synthesis. 2001; pp 5-55.
7. Repka, L. M.; Ni, J.; Reisman, S. E., Enantioselective Synthesis of Pyrroloindolines by a Formal [3 + 2] Cycloaddition Reaction. *J. Am. Chem. Soc.* **2010**, *132*, 14418-14420.
8. Semenov, S. N.; Belding, L.; Cafferty, B. J.; Mousavi, M. P. S.; Finogenova, A. M.; Cruz, R. S.; Skorb, E. V.; Whitesides, G. M., Auto-catalytic Cycles in a Copper-Catalyzed Azide-Alkyne Cycloaddition Reaction. *J. Am. Chem. Soc.* **2018**, *140*, 10221-10232.
9. Chopin, N.; Gérard, H.; Chataigner, I.; Piettre, S. R., Benzofurans as Efficient Dienophiles in Normal Electron Demand [4 + 2] Cycloadditions. *J. Org. Chem.* **2009**, *74*, 1237-1246.
10. Essers, M.; Mück-Lichtenfeld, C.; Haufe, G., Diastereoselective Diels-Alder Reactions of α -Fluorinated α,β -Unsaturated Carbonyl Compounds: Chemical Consequences of Fluorine Substitution. 2. *J. Org. Chem.* **2002**, *67*, 4715-4721.
11. Xiao, W.; Yang, Q.-Q.; Chen, Z.; Ouyang, Q.; Du, W.; Chen, Y.-C., Regio- and Diastereodivergent [4 + 2] Cycloadditions with Cyclic 2,4-Dienones. *Org. Lett.* **2018**, *20*, 236-239.
12. Bartko, S. G.; Hamzik, P. J.; Espindola, L.; Gomez, C.; Danheiser, R. L., Synthesis of Highly Substituted Pyridines via [4 + 2] Cycloadditions of Vinylallenes and Sulfonyl Cyanides. *J. Org. Chem.* **2020**, *85*, 548-563.
13. Lu, Q.; Huang, X.; Song, G.; Sun, C.-M.; Jasinski, J. P.; Keeley, A. C.; Zhang, W., Sequential [3 + 2] and [4 + 2] Cycloadditions for Stereoselective Synthesis of a Novel Polyheterocyclic Scaffold. *ACS Comb. Sci.* **2013**, *15*, 350-355.
14. Collin, G.; Höke, H.; Greim, H., Naphthalene and Hydronaphthalenes. In *Ullmann's encycl. ind. chem.*, 2003.
15. Bird, C. W., The relationship of classical and magnetic criteria of aromaticity. *Tetrahedron* **1996**, *52*, 9945-9952.
16. Remy, R.; Bochet, C. G., Arene-Alkene Cycloaddition. *Chem. Rev.* **2016**, *116*, 9816-9849.
17. Jones, W. H.; Mangold, D.; Plieninger, H., Diensynthesen unter hohem druck. *Tetrahedron* **1962**, *18*, 267-272.
18. Takeda, K. i.; Hagishita, S.; Sugiura, M.; Kitahonoki, K.; Ban, I.; Miyazaki, S.; Kuriyama, K., Diels-Alder reaction—IX: The reaction of 1,7-, 2,7-, 2,6-, and 1,6-dihydroxynaphthalene and 6-bromo-2-naphthol with maleic anhydride and the resolution of some derivatives of the adducts. *Tetrahedron* **1970**, *26*, 1435-1451.
19. Fang, Y.; Murase, T.; Fujita, M., Cavity-promoted Diels-Alder Reactions of Unsubstituted Naphthalene: Fine Reactivity Tuning by Cavity Shrinkage. *Chem. Lett.* **2015**, *44*, 1095-1097.
20. Murase, T.; Horiuchi, S.; Fujita, M., Naphthalene Diels-Alder in a Self-Assembled Molecular Flask. *J. Am. Chem. Soc.* **2010**, *132*, 2866-2867.
21. Kiselev, V. D.; Kashaeva, E. A.; Potapova, L. N.; Iskhakova, G. G., Diels-Alder reaction between naphthalene and N-phenylmaleimide under mild conditions. *Russ. Chem. Bull.* **2004**, *53*, 51-54.
22. Hagiwara, K.; Iwatsu, M.; Urabe, D.; Inoue, M., N-(2,3,4,5,6-pentafluorophenyl)maleimide as a Powerful Dienophile in Dearomatizing Diels-alder Reaction. *Heterocycles* **2015**, *90*, 659-672.
23. Southgate, E. H.; Pospech, J.; Fu, J.; Holycross, D. R.; Sarlah, D., Dearomative dihydroxylation with arenophiles. *Nat. Chem.* **2016**, *8*, 922-928.
24. Breton, G. W.; Newton, K. A., Further Studies of the Thermal and Photochemical Diels-Alder Reactions of N-Methyl-1,2,4-triazoline-3,5-dione (MeTAD) with Naphthalene and Some Substituted Naphthalenes. *J. Org. Chem.* **2000**, *65*, 2863-2869.
25. Kloetzel, M. C.; Herzog, H. L., Polymethyl Aromatic Hydrocarbons. IV. The Reaction of Alkyl naphthalenes with Maleic Anhydride I. *J. Am. Chem. Soc.* **1950**, *72*, 1991-1995.
26. Hernandez, L. W.; Pospech, J.; Klöckner, U.; Bingham, T. W.; Sarlah, D., Synthesis of (+)-Pancreatistatins via Catalytic Desymmetrization of Benzene. *J. Am. Chem. Soc.* **2017**, *139*, 15656-15659.

27. Chan, A. Y.; Perry, I. B.; Bissonnette, N. B.; Buksh, B. F.; Edwards, G. A.; Frye, L. I.; Garry, O. L.; Lavagnino, M. N.; Li, B. X.; Liang, Y.; Mao, E.; Millet, A.; Oakley, J. V.; Reed, N. L.; Sakai, H. A.; Seath, C. P.; MacMillan, D. W. C., Metallaphotoredox: The Merger of Photoredox and Transition Metal Catalysis. *Chem. Rev.* **2022**, *122*, 1485-1542.
28. Döpp, D.; Memarian, H. R., Photo Diels-Alder Additions, VI 1,4-Photoadditions of α -Morpholinoacrylonitrile to 1-Acyl-naphthalenes. *Chem. Ber.* **1990**, *123*, 315-319.
29. Kishikawa, K.; Akimoto, S.; Kohmoto, S.; Yamamoto, M.; Yamada, K., Intramolecular photo[4+2]cycloaddition of an enone with a benzene ring. *J. Chem. Soc., Perkin Trans. I.* **1997**, 77-84.
30. Ma, J.; Strieth-Kalthoff, F.; Dalton, T.; Freitag, M.; Schwarz, J. L.; Bergander, K.; Daniliuc, C.; Glorius, F., Direct Dearomatization of Pyridines via an Energy-Transfer-Catalyzed Intramolecular [4+2] cycloaddition. *Chem* **2019**, *5*, 2854-2864.
31. Morofuji, T.; Nagai, S.; Chitose, Y.; Abe, M.; Kano, N., Protonation-Enhanced Reactivity of Triplet State in Dearomative Photocycloaddition of Quinolines to Olefins. *Org. Lett.* **2021**, *23*, 6257-6261.
32. Strieth-Kalthoff, F.; James, M. J.; Teders, M.; Pitzer, L.; Glorius, F., Energy transfer catalysis mediated by visible light: principles, applications, directions. *Chem. Soc. Rev.* **2018**, *47*, 7190-7202.
33. Ma, J.; Chen, S.; Bellotti, P.; Guo, R.; Schäfer, F.; Heusler, A.; Zhang, X.; Daniliuc, C.; Brown, M. K.; Houk, K. N.; Glorius, F., Photochemical intermolecular dearomative cycloaddition of bicyclic azaarenes with alkenes. *Science* **2021**, *371*, 1338-1345.
34. Zhu, M.; Xu, H.; Zhang, X.; Zheng, C.; You, S.-L., Visible-Light-Induced Intramolecular Double Dearomative Cycloaddition of Arenes. *Angew. Chem. Int. Ed.* **2021**, *60*, 7036-7040.
35. James, M. J.; Schwarz, J. L.; Strieth-Kalthoff, F.; Wibbeling, B.; Glorius, F., Dearomative Cascade Photocatalysis: Divergent Synthesis through Catalyst Selective Energy Transfer. *J. Am. Chem. Soc.* **2018**, *140*, 8624-8628.
36. Hölzl-Hobmeier, A.; Bauer, A.; Silva, A. V.; Huber, S. M.; Bannwarth, C.; Bach, T., Catalytic deracemization of chiral allenes by sensitized excitation with visible light. *Nature* **2018**, *564*, 240-243.
37. Singh, K.; Staig, S. J.; Weaver, J. D., Facile Synthesis of Z-Alkenes via Uphill Catalysis. *J. Am. Chem. Soc.* **2014**, *136*, 5275-5278.
38. Cheng, Q.; Chen, J.; Lin, S.; Ritter, T., Allylic Amination of Alkenes with Iminothianthrenes to Afford Alkyl Allylamines. *J. Am. Chem. Soc.* **2020**, *142*, 17287-17293.
39. Zhang, X.; Rovis, T., Photocatalyzed Triplet Sensitization of Oximes Using Visible Light Provides a Route to Nonclassical Beckmann Rearrangement Products. *J. Am. Chem. Soc.* **2021**, *143*, 21211-21217.
40. Tröster, A.; Bauer, A.; Jandl, C.; Bach, T., Enantioselective Visible-Light-Mediated Formation of 3-Cyclopropylquinolones by Triplet-Sensitized Deracemization. *Angew. Chem. Int. Ed.* **2019**, *58*, 3538-3541.
41. Skubi, K. L.; Kidd, J. B.; Jung, H.; Guzei, I. A.; Baik, M.-H.; Yoon, T. P., Enantioselective Excited-State Photoreactions Controlled by a Chiral Hydrogen-Bonding Iridium Sensitizer. *J. Am. Chem. Soc.* **2017**, *139*, 17186-17192.
42. Zhou, Q. Q.; Zou, Y. Q.; Lu, L. Q.; Xiao, W. J., Visible-Light-Induced Organic Photochemical Reactions through Energy-Transfer Pathways. *Angew. Chem. Int. Ed.* **2019**, *58*, 1586-1604.
43. Singh, A.; Fennell, C. J.; Weaver, J. D., Photocatalyst size controls electron and energy transfer: selectable E/Z isomer synthesis via C-F alkenylation. *Chem. Sci.* **2016**, *7*, 6796-6802.
44. Patra, T.; Das, M.; Daniliuc, C. G.; Glorius, F., Metal-free photosensitized oxyamination of unactivated alkenes with bifunctional oxime carbonates. *Nat. Catal.* **2021**, *4*, 54-61.
45. Patra, T.; Bellotti, P.; Strieth-Kalthoff, F.; Glorius, F., Photosensitized Intermolecular Carboimination of Alkenes through the Persistent Radical Effect. *Angew. Chem. Int. Ed.* **2020**, *59*, 3172-3177.
46. Kleinmans, R.; Pinkert, T.; Dutta, S.; Paulisch, T. O.; Keum, H.; Daniliuc, C. G.; Glorius, F., Intermolecular $[2\pi+2\sigma]$ -photocycloaddition enabled by triplet energy transfer. *Nature* **2022**, 477-482.
47. Daub, M. E.; Jung, H.; Lee, B. J.; Won, J.; Baik, M.-H.; Yoon, T. P., Enantioselective [2+2] Cycloadditions of Cinnamate Esters: Generalizing Lewis Acid Catalysis of Triplet Energy Transfer. *J. Am. Chem. Soc.* **2019**, *141*, 9543-9547.
48. Zheng, J.; Swords, W. B.; Jung, H.; Skubi, K. L.; Kidd, J. B.; Meyer, G. J.; Baik, M.-H.; Yoon, T. P., Enantioselective Intermolecular Excited-State Photoreactions Using a Chiral Ir Triplet Sensitizer: Separating Association from Energy Transfer in Asymmetric Photocatalysis. *J. Am. Chem. Soc.* **2019**, *141*, 13625-13634.
49. Miller, Z. D.; Lee, B. J.; Yoon, T. P., Enantioselective Crossed Photocycloadditions of Styrenic Olefins by Lewis Acid Catalyzed Triplet Sensitization. *Angew. Chem. Int. Ed.* **2017**, *56*, 11891-11895.
50. Plaza, M.; Jandl, C.; Bach, T., Photochemical Deracemization of Allenes and Subsequent Chirality Transfer. *Angew. Chem. Int. Ed.* **2020**, *59*, 12785-12788.
51. Großkopf, J.; Kratz, T.; Rigotti, T.; Bach, T., Enantioselective Photochemical Reactions Enabled by Triplet Energy Transfer. *Chem. Rev.* **2022**, *122*, 1626-1653.
52. Molloy, J. J.; Schäfer, M.; Wienhold, M.; Morack, T.; Daniliuc, C. G.; Gilmour, R., Boron-enabled geometric isomerization of alkenes via selective energy-transfer catalysis. *Science* **2020**, *369*, 302-306.
53. Zhu, C.; Yue, H.; Maity, B.; Atodiresei, I.; Cavallo, L.; Rueping, M., A multicomponent synthesis of stereodefined olefins via nickel catalysis and single electron/triplet energy transfer. *Nat. Catal.* **2019**, *2*, 678-687.
54. Blum, T. R.; Miller, Z. D.; Bates, D. M.; Guzei, I. A.; Yoon, T. P., Enantioselective photochemistry through Lewis acid catalyzed triplet energy transfer. *Science* **2016**, *354*, 1391-1395.
55. Jiang, X.; Li, E.; Chen, J.; Huang, Y., Photo-induced energy transfer relay of N-heterocyclic carbene catalysis: an asymmetric α -fluorination/isomerization cascade. *Chem. Commun.* **2021**, *57*, 729-732.
56. Zhou, Q.-Q.; Zou, Y.-Q.; Lu, L.-Q.; Xiao, W.-J., Visible-Light-Induced Organic Photochemical Reactions through Energy-Transfer Pathways. *Angew. Chem. Int. Ed.* **2019**, *58*, 1586-1604.
57. Wu, L.; Huang, C.; Emery, B. P.; Sedgwick, A. C.; Bull, S. D.; He, X.-P.; Tian, H.; Yoon, J.; Sessler, J. L.; James, T. D., Förster resonance energy transfer (FRET)-based small-molecule sensors and imaging agents. *Chem. Soc. Rev.* **2020**, *49*, 5110-5139.
58. Nevesely, T.; Wienhold, M.; Molloy, J. J.; Gilmour, R., Advances in the E \rightarrow Z Isomerization of Alkenes Using Small Molecule Photocatalysts. *Chem. Rev.* **2022**, *122*, 2650-2694.
59. Huang, M.; Zhang, L.; Pan, T.; Luo, S., Deracemization through photochemical E/Z isomerization of enamines. *Science* **2022**, *375*, 869-874.
60. Strieth-Kalthoff, F.; Glorius, F., Triplet Energy Transfer Photocatalysis: Unlocking the Next Level. *Chem* **2020**, *6*, 1888-1903.
61. Wearing, E. R.; Blackmun, D. E.; Becker, M. R.; Schindler, C. S., 1- and 2-Azetines via Visible Light-Mediated [2 + 2]-Cycloadditions of Alkynes and Oximes. *J. Am. Chem. Soc.* **2021**, *143*, 16235-16242.
62. Becker, M. R.; Wearing, E. R.; Schindler, C. S., Synthesis of azetidines via visible-light-mediated intermolecular [2+2] photocycloadditions. *Nat. Chem.* **2020**, *12*, 898-905.

63. CCDC-2173728 (*endo-3*), CCDC-2173729 (*endo-7*), CCDC-2173850 (*endo-31*), CCDC-2173723 (*exo-31*) contain the supplementary crystallographic data.
64. Guo, R.; Chang, Y.-C.; Herter, L.; Salome, C.; Braley, S. E.; Fessard, T. C.; Brown, M. K., Strain-Release $[2\pi + 2\sigma]$ Cycloadditions for the Synthesis of Bicyclo[2.1.1]hexanes Initiated by Energy Transfer. *J. Am. Chem. Soc.* **2022**, *144*, 7988-7994.